Original Research Article

MHD Natural Convection Casson Fluid Flow over a Non-Isothermal Stretching Sheet Embedded in a Porous Medium

c

Abstract

In the present study, Magnetohydrodynamics (MHD) natural convection casson fluid flow over a non-isothermal stretching sheet embedded in a porous medium is considered. The set of governing differential equations are simplified by similarity variables into coupled ordinary differential equations. The defined stream functions satisfied the continuity equation. Roseland approximation is utilized and the present study is therefore limited to an optically thick fluid. The transformed set of coupled nonlinear ordinary differential equations are then solved numerically via spectral homotopy analysis method (SHAM). Results revealed that the Magnetic parameter (M) reduces the velocity profile but produce a significant increase in the temperature profile. Also, it is observed that increasing the thermal radiation parameter increases the thermal condition of the fluid

Keyword-MHD, Porous medium, SHAM, Viscous, Incompressible, Heat Transfer, Natural Convection.

1. Introduction

Problems in engineering and scientific disciplines are majorly described by partial differential equations (PDEs). These problems are complex and are difficult to solve analytically. Many great authors in the past have developed numerous numerical techniques in solving such problems. The basic celebrated equations which govern flow model in fluid mechanics are the conservation of mass, the conservation of momentum, and the conservation of energy. Many researchers have developed various kinds of fluid flow model based on the above celebrated equations. Mondal et al.[1] analyzed the effect of thermal radiation on an unsteady MHD Axisymmetric stagnation-point flow over a shrinking sheet in presence of temperature dependent thermal conductivity with Navier slip. Metri et al.[2] also discussed thin film flow and heat transfer over an unsteady stretching sheet with thermal radiation internal heating in presence of external magnetic field. Spectral relaxation method for entropy generation on a MHD flow and heat transfer of a Maxwell fluid has been investigated by Shateyi et al.[3]. Shateyi and Makinde[4] analyzed extensively hydrodynamic stagnation-point flow towards a radially stretching convective heated disk.

Fluid flow through porous medium finds applications in engineering such as irrigation, tribology and lubrication, solidification, chromatography etc. Convection flow through porous medium has attracted the attention of researchers in fluid mechanics. Sharma and Aich[5] presented Soret and Dufour effects on steady MHD flow in presence of heat source through a porous medium over a non-isothermal stretching sheet. Fagbade et al.[6] studied influence of magnetic field, viscous dissipation and thermophoresis on Darcy-Forcheimer mixed convection flow in fluid saturated porous media. Heat and mass transfer in visco-elastic fluid through rotating porous channel with hall effect was investigated by Gaur and Jha[7]. Ahmed et al.[8] presented numerical/Laplace transform analysis for MHD radiating heat/mass transport in a Darcian porous regime bounded by an oscillating vertical surface. In the same vein, Shateyi and Marewo[9] presented numerical analysis of unsteady MHD flow near a stagnation point of a two-dimensional porous body with heat and mass transfer, thermal radiation and chemical reaction.

The study of Non-Newtonian fluids is gaining much interest in recent years due to their applications in many engineering industries. Ajayi et al.[10] recently considered viscous dissipation effect on the motion of casson fluid

*

over an upper horizontal thermally stratified melting surface of a paraboloid of revolution. Ullah et al.[11] studied MHD natural convection flow of Nanofluid over nonlinear stretching sheet through porous medium with chemical reaction and thermal radiation. Vijaya et al.[12] studied magnetic field on the flow and heat transfer in a casson thin film on an unsteady stretching surface in the presence of viscous and internal heating. Jithender et al.[13] studied influence of viscous dissipation on unsteady MHD natural convective flow of casson fluid over an oscillating vertical plate via FEM.

Magnetohydrodynamics (MHD) is the study of motion of an electrically conducting fluid as a result of an applied magnetic field. This word magnetohydrodynamics can be split into three as Magneto-Hydro-Dynamics where magneto means magnetic field, hydro means liquid, dynamics means movement. Magnetohydrodynamics has numerous applications in engineering and biological sciences such as the generation of electrical power with the help of an electrically conducting fluid through a magnetic field, in describing the rheological behaviour of blood, plasma confinement, and electromagnetic casting, etc. Due to the numerous applications of MHD mentioned above many researchers finds its importance in fluid dynamics. Rao et al.[14] explored MHD transient free convection and chemically reactive flow past a porous vertical plate with radiation and temperature gradient dependent heat source in slip flow regime. Mahender and Rao[15] has investigated unsteady MHD free convection and mass transfer flow past a porous vertical plate in presence of viscous dissipation. Ahmed and Das[16] examined MHD mass transfer flow past a vertical porous plate embedded in a porous medium in a slip flow regime with thermal radiation and chemical reaction. Rashidi et al.[17] presented free convective heat and mass transfer for MHD fluid flow over a permeable vertical stretching sheet in the presence of the radiation and buoyancy effects.

Heat transfer describes temperature and the flow of heat. It is everyday experience for heat to flow from a hot object to a cold object. Many researchers investigated the importance of heat transfer in fluid dynamics. Mahbub et al.[18] studied soret-dufour effects on the MHD flow and heat transfer of micro-rotation fluid over a nonlinear stretching plate in the presence of suction. Makinde and Onyejekwe[19] presented a numerical study of MHD generalized couette flow and heat transfer with variable viscosity and electrical conductivity. In another study, Idowu et al.[20] presented numerical solution for thermal radiation effect on inclined magnetic field of MHD free convective heat transfer dissipative fluid flow past a moving vertical porous plate with variable suction. Heat transfer effects on a viscous dissipative fluid flow past vertical plate in the presence of induced magnetic field has been studied by Raju et al.[21]. Ahmad[22] explore visco-elastic boundary layer flow past a stretching plate and heat transfer with variable thermal conductivity.

The Spectral homotopy analysis method (SHAM) is the discrete version of the homotopy analysis method (HAM). HAM was first introduced by Liao[23] and he is credited for developing the method. In 2010, Motsa et al.[24] suggested SHAM with the use of Chebyshev pseudo-spectral method to solve linear high order deformation equations. The benefits of these newly proposed method (SHAM) are better accuracy, it requires few iterations, it has less computational effort. It worth mentioning in the present study that the spectral homotopy analysis method (SHAM) is applicable to systems of nonlinear ordinary differential equations and partial differential equations. Numerous researchers used this method in solving problems in fluid dynamics among which we mention in this research work those by (Makukula and Motsa[25]; Atabakan et al.[26]; Makukula et al.[27]; Makukula et al.[28]; Zou et al.[29]; Shaban et al.[30]; Shateyi and Motsa[31])

In all the literatures discussed above and to the very best of our knowledge, no study or little attention has been on MHD natural convection casson fluid flow over a non-Isothermal stretching sheet embedded in a porous medium. The novelty of our work is to present the analysis of Casson fluid flow over a non-isothermal stretching sheet embedded in a porous medium. Effects of parameters such as thermal radiation, magnetic field, Joule heating and heat generation are considered significant in the present study. An elegance and accurate numerical method called spectral homotopy analysis method is utilized in solving the present modeled equations.

2. Mathematical Formulation

Consider a steady, incompressible, viscous, MHD two-dimensional boundary layer flow over a non-isothermal stretching sheet embedded in a porous medium. The stretching sheet is placed at the bottom of the fluid porous medium with the effects of heat generation and radiation [see Fig 1]. The Rosseland approximation is considered and the fluid is assumed to be optically thin. A magnetic field of uniform strength (B_0) is executed transverse to the sheet. The induced magnetic field is neglected because we assumed the magnetic Reynolds number to be small. We take x-axis along the sheet and y-axis normal to it. The rheological equation of state for the isotropic and

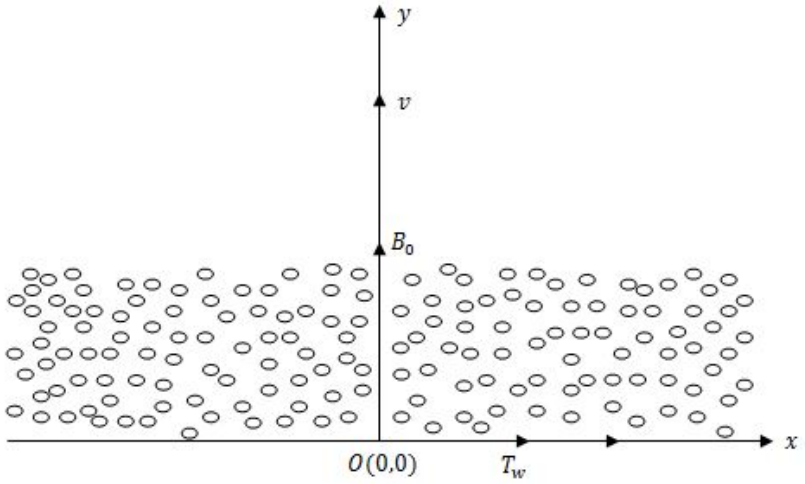

Figure 1: Physical Model

incompressible flow of a casson fluid is given by Mukhopadhylay[32] as:

$$\tau_{ij} = 2(\mu_B + \frac{p_y}{\sqrt{2\pi}})e_{ij} \quad , \pi > \pi_c \tag{1}$$

$$\tau_{ij} = 2(\mu_B + \frac{p_y}{\sqrt{2\pi_c}})e_{ij} \quad , \pi < \pi_c \tag{2}$$

As a result of the Boussineq's approximation and the basic assumptions made above, the equations governing the flow model can be written as:
Continuity equation

$$\frac{\partial u}{\partial x} + \frac{\partial v}{\partial y} = 0 \tag{3}$$

Momentum equation

$$u\frac{\partial u}{\partial x} + v\frac{\partial v}{\partial y} = \nu\left(1 + \frac{1}{\beta}\right)\frac{\partial^2 u}{\partial y^2} - \frac{\nu}{k}u - \frac{\sigma B_0^2}{\rho}u \tag{4}$$

Energy equation

$$u\frac{\partial T}{\partial x} + v\frac{\partial T}{\partial y} = \frac{k}{\rho c_p}\frac{\partial^2 T}{\partial y^2} - \frac{1}{\rho c_p}\frac{\partial q_r}{\partial y} + \frac{\sigma B_0^2}{\rho c_p}u^2 + \frac{\mu}{\rho c_p}\left(1 + \frac{1}{\beta}\right)(\frac{\partial u}{\partial y})^2 + \frac{Q(T - T_\infty)}{\rho c_p} \tag{5}$$

subject to the boundary conditions:

$$u = cx \quad , v = 0 \quad , T = T_w(x) = T_\infty + \frac{Dx^2}{l^2}\theta(\eta) \quad as \quad y = 0 \tag{6}$$

$$u \longrightarrow 0 \quad , T \longrightarrow T_\infty \quad at \quad y \longrightarrow \infty \tag{7}$$

where u and v are fluid velocity components in x and y directions respectively, ν is the fluid viscosity, σ is the electrical conductivity, B_0 is the applied magnetic field, ρ is the density of the fluid, T is the fluid temperature, T_∞ is the free stream temperature, c_p is the specific heat at constant pressure, Q is heat generation term, k is the permeability term. The first term $\nu\frac{\partial^2 u}{\partial y^2}$ on the RHS of the momentum equation is the viscous term, the second term $\frac{\nu}{k}u$ is the porous term, while the term $\frac{\sigma B_0^2}{\rho}u$ is the magnetic field term. It is noticed that the magnetic term

opposes the flow. In the energy equation, the convection term is $u\frac{\partial T}{\partial x}$. This term is responsible for the distribution of temperature. The diffusion term is $\frac{k}{\rho c_p}\frac{\partial^2 T}{\partial y^2}$, the radiative term is $\frac{1}{\rho c_p}\frac{\partial q_r}{\partial y}$. We assumed in the present study that the radiative flux that dominate the flow is $\frac{\partial q_r}{\partial y}$ and due to this we neglect the x-direction radiative flux $\frac{\partial q_r}{\partial x}$. The term $\frac{\sigma B_0^2}{\rho c_p}u^2$ is the joule heating term. The term $\frac{\mu}{\rho c_p}(\frac{\partial u}{\partial y})^2$ is the viscous dissipation term and the heat generation term is $\frac{Q(T-T_\infty)}{\rho c_p}$

With the stream function defined as $u = \frac{\partial \Psi}{\partial y}$ and $v = -\frac{\partial \Psi}{\partial x}$, the governing equations becomes:

$$\frac{\partial^2 \Psi}{\partial x \partial y} - \frac{\partial^2 \Psi}{\partial y \partial x} = 0 \tag{8}$$

$$\frac{\partial \Psi}{\partial y}\frac{\partial^2 \Psi}{\partial x \partial y} - \frac{\partial \Psi}{\partial x}\frac{\partial^2 \Psi}{\partial x \partial y} = \nu\left(1+\frac{1}{\beta}\right)\frac{\partial^3 \Psi}{\partial y^3} - \frac{\nu}{k}\frac{\partial \Psi}{\partial y} - \frac{\sigma B_0^2}{\rho}\frac{\partial \Psi}{\partial y} \tag{9}$$

$$\frac{\partial \Psi}{\partial y}\frac{\partial T}{\partial x} - \frac{\partial \Psi}{\partial x}\frac{\partial T}{\partial y} = \frac{k}{\rho c_p}\frac{\partial^2 T}{\partial y^2} - \frac{1}{\rho c_p}\frac{\partial q_r}{\partial y} + \frac{\sigma B_0^2}{\rho c_p}(\frac{\partial \Psi}{\partial y})^2 + \frac{\mu}{\rho c_p}\left(1+\frac{1}{\beta}\right)(\frac{\partial^2 u}{\partial y^2})^2 + \frac{Q(T-T_\infty)}{\rho c_p} \tag{10}$$

subject to the boundary conditions:

$$\frac{\partial \Psi}{\partial y} = cx \ , \frac{\partial \Psi}{\partial x} = 0 \ , T = T_w(x) = T_\infty + \frac{Dx^2}{l^2}\theta(\eta) \quad as \quad y = 0 \tag{11}$$

$$\frac{\partial \Psi}{\partial y} \longrightarrow 0 \ , T \longrightarrow T_\infty \quad at \quad y \longrightarrow \infty \tag{12}$$

Obviously from Eq (8) the stream function satisfied the continuity equation. Utilizing the Roseland model, the radiative heat flux as reported by Fagbade et al.[33] is defined as:

$$q_r = -\frac{-4\sigma^*}{3k^*}\frac{\partial T^4}{\partial y} \tag{13}$$

The temperature difference within the flow is assumed to be sufficiently small and T^4 could be expressed as a linear function of temperature T_∞ by truncating in Taylor's series about k_0 as described below;

$$T(k) = T(k_0) + (k-k_0)T'(k_0) + \frac{(k-k_0)^2}{2!}T''(k_0) + ... + \frac{(k-k_0)^n}{2!}T^n(k_0) \tag{14}$$

Neglecting higher order in the equation above result to

$$T^4 \approxeq 4T_\infty^3 T - 3T_\infty^4 \tag{15}$$

Invoking Eqs. (13) and (15) on (5), the energy equation becomes:

$$u\frac{\partial T}{\partial x} + v\frac{\partial T}{\partial y} = \frac{k}{\rho c_p}\frac{\partial^2 T}{\partial y^2} + \frac{16\sigma^* T_\infty^3}{3\rho c_p k_e}\frac{\partial^2 T}{\partial y^2} + \frac{\sigma B_0^2}{\rho c_p}u^2 + \frac{\mu}{\rho c_p}\left(1+\frac{1}{\beta}\right)\left(\frac{\partial u}{\partial y}\right)^2 + \frac{Q(T-T_\infty)}{\rho c_p} \tag{16}$$

simplifying further yields:

$$u\frac{\partial T}{\partial x} + v\frac{\partial T}{\partial y} = \frac{1}{\rho c_p}\frac{\partial^2 T}{\partial y^2}(k + \frac{16\sigma^* T_\infty^3}{3k_e}) + \frac{\sigma B_0^2}{\rho c_p}u^2 + \frac{\mu}{\rho c_p}(1+\frac{1}{\beta})(\frac{\partial u}{\partial y})^2 + \frac{Q(T-T_\infty)}{\rho c_p} \tag{17}$$

To transform the governing Eqs. (3)-(5), the following similarity transformations are introduced

$$\Psi = \sqrt{c\nu}xf(\eta) \ , \eta = \sqrt{\frac{c}{\nu}}y \ , \theta(\eta) = \frac{T-T_\infty}{T_w - T_\infty} \ , T = T_\infty + D\frac{x^2}{l^2}\theta(\eta) \tag{18}$$

In view of Eq (18), the momentum and the energy equations are reduced to the following coupled nonlinear ordinary differential equations;

$$\left(1+\frac{1}{\beta}\right)f''' - \left(\frac{1}{k_p} + M^2\right)f' + ff'' + f'^2 = 0 \tag{19}$$

$$\left(1+\frac{4}{3}Ra\right)\theta'' - 2Prf'\theta + Prf\theta' + PrM^2Ecf'^2 + PrEc\left(1+\frac{1}{\beta}\right)f''^2 + Pr\Delta\theta = 0 \tag{20}$$

subject to:

$$f = 0 \ , f' = 1 \ , \theta = 1 \quad , at \quad \eta = 0 \tag{21}$$

$$f'(\infty) = 0 \quad , \theta(\infty) = 0 \quad as \quad \eta \longrightarrow \infty \tag{22}$$

where
$Pr = \frac{\nu \rho c_p}{k} \ , k_p = \frac{ck}{\nu} \ , M = \left(\frac{\sigma B_0^2}{\rho c_p}\right) \ , Ec = \frac{c^2 l^2}{c_p D} \ , \Delta = \frac{Q}{\rho c_p c}, \ Ra = \frac{4\sigma^* T_\infty^3}{k k_e}$
are the Prandtl number, Permeability parameter, magnetic parameter, Eckert number, heat generation parameter and thermal radiation parameter.

3. Spectral Homotopy Analysis Method (SHAM)

SHAM is the numerical version of homotopy analysis method (HAM) proposed by Liao[23]. SHAM is discussed extensively in the investigation of Motsa et al.[24]. In spectral homotopy analysis method, the linearized equations are solved using the Chebyshev spectral collocation method. Many researchers preferred spectral methods than other numerical method because of their accuracy, it requires few iterations and it is very easy to compute. The SHAM requires that the nonlinear equations under investigation is split into linear and nonlinear parts. In implementing SHAM, we first transform the domain of the problem from $[0, 1]$ to $[-1, 1]$ using the algebraic mapping defined below:

$$\xi = \frac{2\eta}{L} - 1 \quad , \xi \in [-1, 1] \tag{23}$$

For easy computation and convenience we make the boundary conditions homogeneous by applying the following transformation

$$f(\eta) = f(\xi) + f_0(\eta) \ , \theta(\eta) = \theta(\xi) + \theta_0(\eta) \tag{24}$$

where $f_0(\eta) = 1 - exp(-\eta) \quad , \theta_0 = exp(-\eta)$ are chosen to satisfy the boundary conditions in Eq. (21) and (22). Substituting (23) and (24) into the transformed governing equations (19)-(20) and boundary conditions (21)-(22), we obtain

$$\left(1 + \frac{1}{\beta}\right) f'''(\xi) + f(\xi) f''(\xi) + \alpha_1 f(\xi) + \alpha_2 f''(\xi) + f'(\xi) f'(\xi) + \alpha_3 f'(\xi) - \left(\frac{1}{k_p} + M^2\right) f'(\xi) = H_1(\eta) \tag{25}$$

$$\left(1 + \frac{4}{3} Ra\right) \theta''(\xi) + Pr f(\xi) \theta'(\xi) + \beta_1 f(\xi) + \beta_2 \theta'(\xi) - 2Pr f'(\xi) \theta(\xi) + \beta_3 f'(\xi) + \beta_4 \theta(\xi) +$$

$$PrM^2 Ec f'(\xi) f'(\xi) + \beta_5 f'(\xi) + PrEc \left(1 + \frac{1}{\beta}\right) f''(\xi) f''(\xi) + \beta_6 f''(\xi) + Pr\Delta\theta(\xi) = H_2(\eta) \tag{26}$$

subject to:

$$f(-1) = f'(1) = 0 \quad , \theta(-1) = \theta(1) = 0 \tag{27}$$

where prime connote differentiation with respect to ξ and we set

$$\alpha_1 = f_0''(\eta), \alpha_2 = f_0(\eta), \alpha_3 = 2f_0'(\eta), H_1(\eta) = -\left(1 + \frac{1}{\beta}\right) f_0'''(\eta) - f_0(\eta) f_0''(\eta) - f_0'(\eta) f_0'(\eta) + \left(\frac{1}{k_p} + M^2\right) f_0',$$

$$\beta_1 = Pr\theta_0'(\eta), \beta_2 = Pr f_0(\eta), \beta_3 = -2Pr\theta_0(\eta), \beta_4 = -2Pr f_0'(\eta), \beta_5 = 2PrM^2 Ec f_0'(\eta), \beta_6 = 2PrEc \left(1 + \frac{1}{\beta}\right) f_0''(\eta),$$

$$H_2(\eta) = -\left(1 + \frac{4}{3} Ra\right) \theta_0''(\eta) - Pr f_0(\eta) \theta'(\eta) + 2Pr f_0'(\eta) \theta_0(\eta) - PrM^2 Ec f_0'(\eta) - PrEc \left(1 + \frac{1}{\beta}\right) f_0''(\eta) f_0''(\eta) - Pr\Delta\theta_0(\eta) \tag{28}$$

In Eqs (25)-(26), the non-homogeneous linear part is given by

$$\left(1+\frac{1}{\beta}\right)f_l'''+\alpha_1 f_l+\alpha_2 f_l''+\alpha_3 f_l'-\left(\frac{1}{k_p}+M^2\right)f_l' \quad = \quad H_1(\eta) \tag{29}$$

$$\left(1+\frac{4}{3}Ra\right)\theta_l''+\beta_1 f_l+\beta_2\theta_l'+\beta_3 f_l'+\beta_4\theta_l+\beta_5 f_l'+\beta_6 f_l''+Pr\Delta\theta_l \quad = \quad H_2(\eta) \tag{30}$$

subject to:

$$f(-1)=f'(1)=0 \quad ,\theta(-1)=\theta(1)=0 \tag{31}$$

Chebyshev pseudospectral method is used to solve (29)-(30). The unknown functions $f_l(\xi),\theta_l(\xi)$ are approximated as a truncated series of chebyshev polynomials of the form:

$$f_l(\xi)\approx f_l^N=\sum_{k=0}^{N} f_k^N T_{1k}(\xi_J) \quad J=0,1,2,...,N \tag{32}$$

$$\theta_l(\xi)\approx \theta_l^N=\sum_{k=0}^{N} \theta_k^N T_{2k}(\xi_J) \quad J=0,1,2,...,N \tag{33}$$

where T_{1k} and T_{2k} are the k^{th} Chebyshev polynomials and their coefficients is given by f_k, and θ_k respectively, $\xi_0,\xi_1,\xi_2,...,\xi_N$ are Gauss-Lobatto collocation point defined by

$$\xi_J=\cos\left(\frac{\pi J}{N}\right), \quad J=0,1,2,...,N \tag{34}$$

where N is the number of collocation points. The derivatives of the function $f_l(\xi)$, and $\theta_l(\xi)$ at all the collocation points are defined as;

$$\frac{d^r f_l}{d\xi^r}=\sum_{k=0}^{N} D_{kJ}^r f_l(\xi_J), \quad \frac{d^r\theta_l}{d\xi^r}=\sum_{k=0}^{N} D_{kJ}^r \theta_l(\xi_J) \tag{35}$$

In Eq. (25) above, r is the order of differentiation, $\mathbf{D}=\frac{2}{L}D$ where D is the Chebyshev spectral differentiation matrix. Invoking Eqs (32)-(35) into Eqs (29)-(30), we have

$$AF_L=G \tag{36}$$

Subject to the boundary conditions

$$f_l(\xi_N)=0,\ \sum_{k=0}^{N} D_{Nk}f_k(\xi_k)=1,\sum_{k=0}^{N} D_{0k}f_k(\xi_k)=0,\ \ \theta_l(\xi_N)=1.\theta_l(\xi_0)=0. \tag{37}$$

where

$$\begin{bmatrix} A_{11} & A_{12} \\ A_{21} & A_{22} \end{bmatrix} \tag{38}$$

$$A_{11}=\left(1+\frac{1}{\beta}\right)D^3+\alpha_1 I+\alpha_2 D^2+\alpha_3 D-\left(\frac{1}{k_p}+M^2\right)D, \ \ A_{12}=0,$$

$$A_{21}=\beta_1+\beta_3 D+\beta_5 D+\beta_6 D^2 \ \ A_{22}=\left(1+\frac{4}{3}Ra\right)D^2+\beta_2 D+\beta_4 I+Pr\Delta \tag{39}$$

And;
$F_l=[f_l(\xi_0),...,f_l(\xi_N),\theta_l(\xi_0),...,\theta_l(\xi_N)]$

$G=[H_l(\eta_0),...,H_l(\eta_N),H_2(\eta_0),...,H_2(\eta_N)]$

$\alpha_i = diag([\alpha_i(\eta_0), ..., \alpha_i(\eta_{N-1}), \alpha_i(\eta_{N-1}, \alpha_i(\eta_N])$

$\beta_i = diag([\beta_i(\eta_0), ..., \beta_i(\eta_{N-1}), \beta_i(\eta_{N-1}, \beta_i(\eta_N])\ \ i = 1, 2, 3$

We delete the first and the last rows and columns of A in other to implement the boundary conditions (37). Also, we imposed the boundary conditions (37) on the first and last rows of the modified matrix A, and setting the modified matrix G to zero, all the values of $f_l(\xi_0), ..., f_l(\xi_N), \theta_l(\xi_0), ..., \theta_l(\xi_N)$ are determined from;

$$F_l = A^{-1}.G \tag{40}$$

Eq. (40) above provide us the initial approximation for the SHAM solution of the governing equations. To sought the SHAM approximate solutions of (25)-(26), we define the following linear operators

$$L_f[\bar{f}(\eta, q), \bar{\theta}(\eta, q)] = \left(1 + \frac{1}{\beta}\right) f''' + \alpha_1 f + \alpha_2 f'' + \alpha_3 f' - \left(\frac{1}{k_p} + M^2\right) f' \tag{41}$$

$$L_\theta[\bar{f}(\eta, q), \bar{\theta}(\eta, q)] = (1 + \frac{4}{3}Ra)\theta'' + \beta_1 f + \beta_2\theta' + \beta_3 f' + \beta_4\theta + \beta_5 f' + \beta_6 f'' + Pr\Delta\theta \tag{42}$$

where $q\epsilon[0, 1]$ is the embedding parameter, $\bar{f}(\eta, q), and \bar{\theta}(\eta, q)$ are the unknown functions. The zeroth order deformation equation are given by

$$(1 - q)L_f[\bar{f}(\eta; q) - f_l(\xi)] = q\hbar_f N_f[\bar{f}(\xi; q), \bar{\theta}(\xi, q)] - H_1, \tag{43}$$

$$(1 - q)L_\theta[\bar{\theta}(\eta; q) - \theta_l(\xi)] = q\hbar_f N_\theta[\bar{f}(\xi; q), \bar{\theta}(\xi, q)] - H_2. \tag{44}$$

Where $\hbar_f, \hbar_\theta$ are non-zero convergence controlling auxillary parameter and $N_{\bar{f}}$ and N_θ are non-linear operations given by:

$$N_f[\bar{f}(\eta, q), \bar{\theta}(\eta, q)] = ff'' + f'f' \tag{45}$$

$$N_\theta[\bar{f}(\eta, q), \bar{\theta}(\eta, q)] = f\theta' - 2Prf'\theta + PrM^2Ecf'f' + PrEc\left(1 + \frac{1}{\beta}\right) f''f'' \tag{46}$$

Differentiating the above equation m-times with respect to q, setting $q = 0$ and dividing the resulting equations by $m!$ yields the m^{th} order deformation equations.

$$L_f[f_m(\xi) - \chi_m f_{m-1}(\xi)] = \hbar_f R_m^f, \tag{47}$$

$$L_\theta[\theta_m(\xi) - \chi_m\theta_{m-1}(\xi)] = \hbar_\theta R_m^\theta. \tag{48}$$

Subject to:

$$f_m(-1) = f'_m(-1) = f'_m(1) = 0, \tag{49}$$

$$\theta_m(-1) = \theta_m(1) = 0. \tag{50}$$

Where;

$$R_m^f(\xi) = \left(1 + \frac{1}{\beta}\right) f'''_{m-1} + \alpha_1 f_{m-1} + \alpha_2 f''_{m-1} + \alpha_3 f'_{m-1} - \left(\frac{1}{k_p} + M^2\right) f'_{m-1} + \sum_{n=0}^{n-1}(f_n f''_{m-1-n} + f'_n f'_{m-1-n}) - H_1(\eta)(1 - X_m), \tag{51}$$

$$R_m^\theta(\xi) = \left(1 + \frac{4}{3}Ra\right)\theta''_{m-1} + \beta_1 f_{m-1} + \beta_2\theta'_{m-1} + \beta_3 f'_{m-1} + \beta_4\theta_{m-1} + \beta_5 f'_{m-1} + \beta_6 f''_{m-1} + Pr\Delta\theta_{m-1} + \sum_{n=0}^{m-1}\left(f_n\theta'_{m-1-n} - 2Prf'_n\theta_{m-1-n} + PrM^2Ecf'_n f'_{m-1-n} + PrEc\left(1 + \frac{1}{\beta}\right) f''_n f''_{m-1-n}\right). \tag{52}$$

Applying Chebyshev pseudo-spectral transformation on above gives;

$$Af_m = (X_m + \hbar)Af_{m-1} - \hbar(1 - X_m)G + \hbar Q_{m-1}$$

subject to the boundary conditions

$$f_m(\xi_N) = 0, \quad f_m(\xi_0) = 0, \tag{53}$$
$$\theta_m(\xi_N) = 0, \quad , \theta_m(\xi_0) = 0. \tag{54}$$

where A and G are defined above

$$F_m = [f_m(\xi_0), f_m(\xi_1), ..., f_m(\xi_N), \theta_m(\xi_0), \theta_m(\xi_1), ..., \theta_m(\xi_N)]^T$$

$$Q_{1,m-1} = \sum_{n=0}^{m-1} [D^2 f_{m-1-n} f_n + D f_n D f_{m-1-n}] \tag{55}$$

$$Q_{2,m-1} = \sum_{n=0}^{m-1} [Pr f_n D\theta_{m-1-n} - 2PrDf_n\theta_{m-1-n} + PrM^2 EcDf_n Df_{m-1-n} + PrEc\left(1 + \frac{1}{\beta}\right) D^2 f_n D^2 f_{m-1-n} \tag{56}$$

The boundary conditions above are implemented on A on the left hand-side in rows $1, N, N+1, (N+1)$ respectively as before with the initial solution above. The corresponding rows, all column of A on the right hand-side $G, Q_{1,m-1}, Q_{2,m-1}$ are all set to zero. This result in the following recursive formular $m \geq 1$

$$F_m = (\chi_m + \hbar)A^{-1}.\bar{A}f_{m-1} + \hbar A^{-1}[Q_{m-1} - (1 + \chi_m)G], \tag{57}$$
$$\Theta_m = (\chi_m + \hbar)A^{-1}.\bar{A}\theta_{m-1} + \hbar A^{-1}[Q_{m-1} - (1 + \chi_m)G] \tag{58}$$

4. Graphs, Results and Discussion

A novel and efficient method called spectral homotopy analysis method (SHAM) was used to solve the set of governing coupled nonlinear ordinary differential equations. The effects of all pertinent flow parameters on the velocity and temperature profile were examined. To get a clear insight to physics of the problem, values of controlling parameters are set as $Pr = 0.71, Gr = 2.0, M = 1.0, k_p = 0.1, R = 0.5, Ec = 0.01, \Delta = 0.1$. All tables and graphs corresponds to the above stated values unless or otherwise stated. It worth mentioning in the present study that all programs for generating solutions were coded in MATLAB R2012a. Our results were generated at $L = 30$ and the number of collocation point at $Nx = 100$ and we observed that if the value is increased there is no changes on the numerical results of the skin-friction and Nusselt number in Table 1 and 2. In table 1, an increase in both viscous dissipation term. Table 2 presents the computed values of thermal radiation parameter. The table implies increase in the radiation parameter intensify the skin-friction coefficient and Nusselt number.

The graphical solution of all controlling flow parameters are presented in figures 2-7. In figure 2 the effects of the magnetic parameter is presented. From the figure 2 it is observed that increase in magnetic parameter leads to decrease in the velocity and temperature profiles respectively. The application of the transverse magnetic field which gives rise to a drag-like or resistive force called Lorentz force slows down the motion of an electrically conducting fluid. It is observed that the resistive force warm the stretching sheet and thereby increases the temperature profile.

The effect of the permeability parameter (k_p) is presented in figure 3. The results revealed that an increase in (k_p) lead to increase in the velocity profile but reduces the temperature profile. Figure 4 presents the effect of Prandtl number (Pr) on the velocity and temperature profiles respectively. It is noted from the figure 4 that increasing the Pr decreases both velocity and temperature profiles. This is because fluids with higher Pr possesses more viscosities and thereby lower the skin-friction. Also, Pr decreases the temperature profile due to small value of Prandtl number say $Pr < 1$ the fluid is highly conducive. The Prandtl number for air is ($Pr = 0.71$) while that of water is ($Pr = 7.0$). Furthermore, when $Pr = 1$ the momentum diffusion rate is beyond thermal diffusion rate. Figure 5 depicted effect of the casson parameter (β) on the velocity and temperature profiles. A significant reduction in the velocity profile is observed as the β is increasing. Increasing β leads to an increase in the fluid dynamic viscosity. Intensifying the casson parameter increases the temperature profile as seen in figure (5).

Increasing the viscous dissipative term i.e Eckert number (Ec) intensifies both the velocity and temperature profiles as presented in figure 6. Ec is the relationship between the kinetic energy in the flow and the enthalpy. Figure 7 presents the effect of heat generation parameter on the velocity and temperature profiles. From figure 7, we discovered that as a result of the generation of heat there is increase the velocity in the boundary layer. Figure 8 displayed the effect of thermal radiation parameter on the temperature and velocity profile respectively. Ra described the contribution of conduction mode of heat transfer to radiation mode of heat transfer. Thermal radiation enhances convective flow. When Ra is increased, there is a significant increase in the thermal condition of fluid and its boundary layer. Also, when thermal radiation is increased, there is enhancement of the heat flux from the plate which increases both velocity and temperature profiles as shown in figure 8.

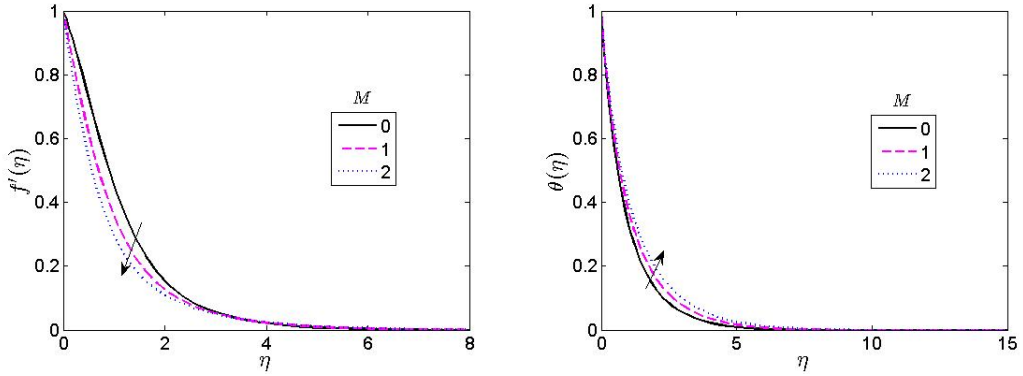

Figure 2: Velocity and Temperature profiles for different values of Magnetic parameter M

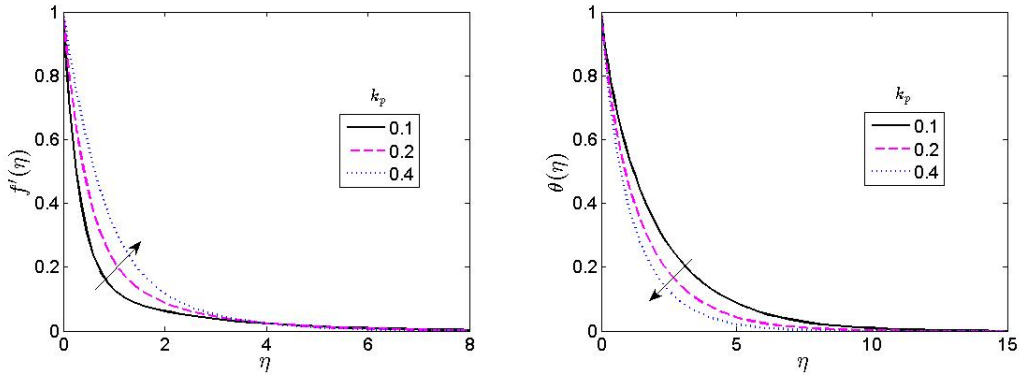

Figure 3: Velocity and Temperature profiles for different values of permeability parameter k_p

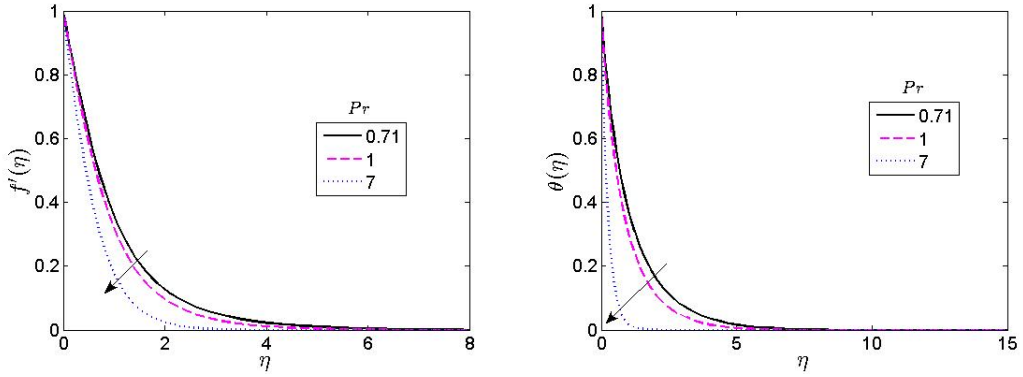

Figure 4: Velocity and Temperature profiles for different values of Prandtl number Pr

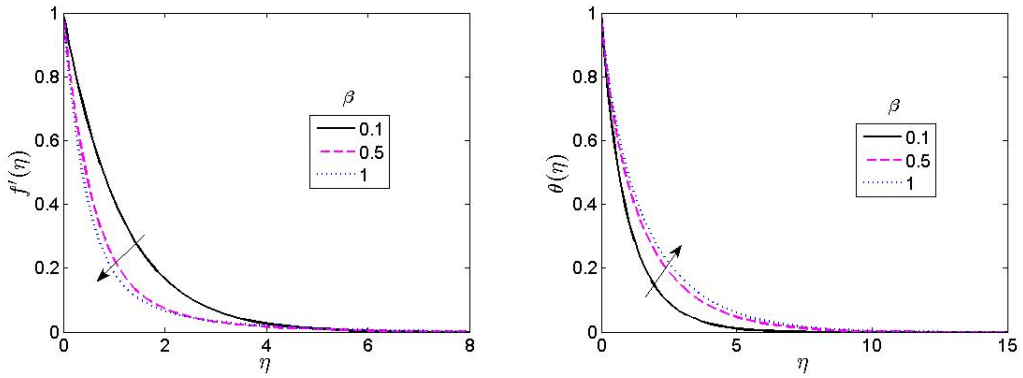

Figure 5: Velocity and Temperature profiles for different values of casson parameter β

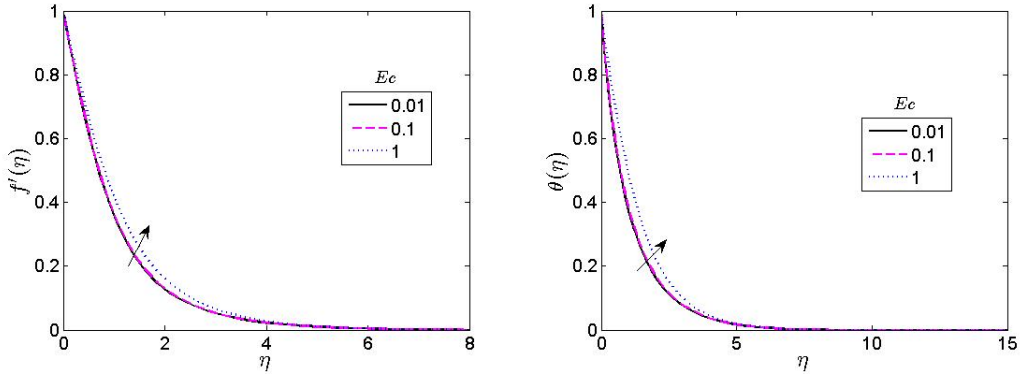

Figure 6: Velocity and Temperature profiles for different values of Eckert number Ec

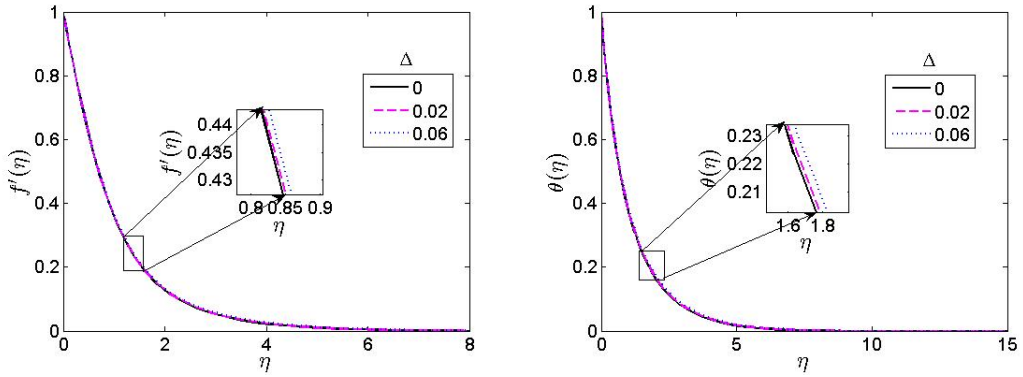

Figure 7: Velocity and Temperature profiles for different values of heat generation parameter Δ

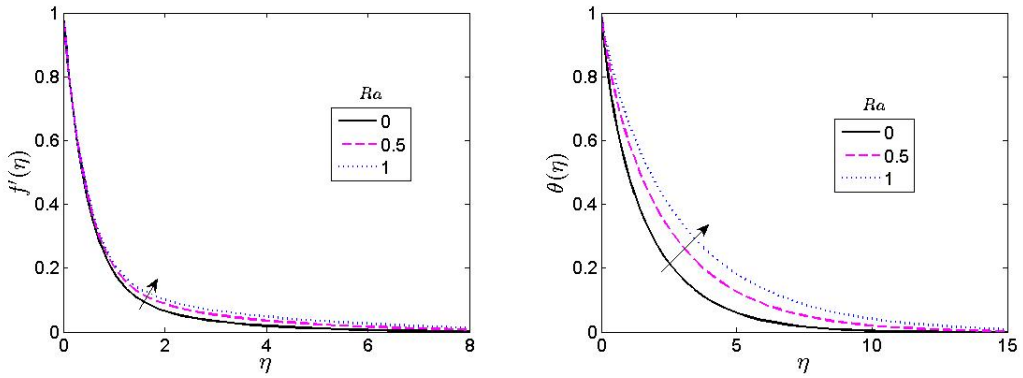

Figure 8: Velocity and Temperature profiles for different values of thermal radiation parameter Ra

Table 1: Computational values of skin friction coefficient Cf and local Nusselt number Nu for different values of Eckert number and casson parameter β for $Pr = 0.71, M = 1.0, k_p = 0.1, Ra = 0.5, \Delta = 0.1$

Ec	β	Cf	Nu
0.01	0	1.65444360	0.91049042
	0.5	1.43163937	0.96027683
	1	1.22060494	1.00476744
0.1	0	1.65444360	0.85841294
	0.5	1.42931715	0.91090667
	1	1.21567661	0.95810125

Table 2: Computational values of skin-friction coefficient Cf and local Nusselt number Nu for different values of thermal radiation parameter Ra for $Pr = 0.71, Gr = 2.0, M = 1.0, k_p = 0.1, \Delta = 0.1$

Ra	$u'(0)$	$-\theta'(0)$
0	0.56326856	0.49095360
0.5	0.65338687	0.65965460
1.0	0.7228686	0.80976786
2.0	0.82725490	1.08571491

5. Conclusion

In the present study, we have accounted for the analysis of the spectral homotopy method (SHAM) for MHD natural convection Casson fluid flow over a non-isothermal stretching sheet embedded in a porous medium.. SHAM adopts the Chebyshev pheudospectral method to solve the system of equations. The SHAM is the numerical version of the proposed method by Liao[23] called homotopy analysis method. The SHAM is an efficient method which is easy to compute and gives accurate results. From our results, the following conclusions were drawn:

- Increasing the Casson parameter (β) decreases the velocity profile and increases the temperature profile.
- The magnetic parameter decreases the velocity profile but increases the temperature profile.
- The effects of heat generation and thermal radiation on the flow is significant and thereby finds application in numerous problems in engineering.

6. References

[1] Mondal S., Haroun A.H. Nageeb, and Sibanda P. (2015): The Effects of Thermal Radiation on an Unsteady MHD Axisymmetric Stagnation-point Flow over a Shrinking Sheet in Presence of Temperature Dependent Thermal Conductivity with Navier Slip. PLOS ONE/DOI:10.1371/journal.pone.0138355, 1-23.

[2] Metri G. P., Tawade J., and Abel S. M. (2016): Thin Film Flow and Heat Transfer Over an Unsteady Stretching Sheet with Thermal Radiation, Internal Heating in Presence of External Magnetic Field. Physics Fluid Dynamics, pp. 1-16.

[3] Shateyi S., Motsa S.S. and Makukula Z. (2015): On Spectral Relaxation Method for Entropy Generation on a MHD Flow and Heat Transfer of Maxwell Fluid. Journal of Applied Fluid Mechanics, 8(1), pp. 21-31.

[4] Shateyi S. and Makinde O.D. (2013): Hydromagnetic Stagnation-point Flow towards a Radially Stretching Convectively Heated Disk. Hindawi Publishing Coorporation, Mathematical Problems in Engineering, pp. 1-8.

[5] Sharma B. R., and Aich A. (2016): Soret and Dufour Effects on Steady MHD Flow in Presence of Heat Source through a Porous Medium Over a Non-isothermal Stretching Sheet. IOSR Journal of Mathematics, 12(1), pp. 53-60.

[6] Fagbade A.I., Falodun B.O., Boneze C.U. (2015): Influence of Magnetic field, Viscous Dissipation and Thermophoresis on Darcy-Fircheimer Mixed Convection Flow in Fluid Saturated Porous Media. American Journal of Computational Mathematics,5, pp. 18-40.

[7] Gaur K. P. and Jha K. A. (2016): Heat and Mass Transfer in Visco-elastic Fluid through Rotating Porous Channel with Hall Effect. Open Journal of Fluid Dynamics, 6, pp. 11-29.

[8] Ahmed S., Abdul B., and Chamkha A.J. (2015): Numerical/Laplace Transform Analysis for MHD Radiating Heat/mass Transport in a Darcian Porous Regime Bounded by an Oscillating Vertical Surface. Alexandria Engineering Journal, 54, pp. 45-54.

[9] Shateyi S. and Marewo G. T., (2014): Numerical Analysis of Unsteady MHD Flow near a Stagnation Point of a Two-dimensional Porous body with Heat and Mass Transfer, Thermal Radiation, and Chemical Reaction. Boundary Value Problems, http://www.boundaryvalueproblems.com/content/2014/1/218, pp. 1-18.

[10] Ajayi T.M., A. J. Omowaye, and I. L. Animasaun (2017). Viscous Dissipation Effects on the Motion of Casson Fluid over an Upper Horizontal Thermally Stratified Melting Surface of a Paraboloid of Revolution: Boundary Layer Analysis, Journal of Applied Mathematics, Article ID 1697135, 13 pages https://doi.org/10.1155/2017/1697135.

[11] Ullah Imran, Ilyas Khan and Sharidan Shafie (2016). MHD Natural Convection Flow of Casson Nanofluid over Nonlinearly Stretching Sheet Through Porous Medium with Chemical Reaction and Thermal Radiation, Nanoscale Research Letters, 11:527 DOI 10.1186/s11671-016-1745-6.

[12] Vijaya, N., Sreelakshmi, K. and Sarojamma, G. (2016) Effect of Magnetic Field on the Flow and Heat Transfer in a Casson Thin Film on an Unsteady Stretching Surface in the Presence of Viscous and Internal Heating. Open Journal of Fluid Dynamics, 6, 303-320. http://dx.doi.org/10.4236/ojfd.2016.64023

[13] Jithender Reddy G, R. Srinivasa Raju , J. Anand Rao (2017) Influence of viscous dissipation on unsteady MHD natural convective flow of Casson fluid over an oscillating vertical plate via FEM. Ain Shams Eng J (2017), (Article in Press) http://dx.doi.org/10.1016/j.asej.2016.10.012

[14] Rao M. B., Reddy V. G., Raju M.C., Varma S.V.K. (2013): MHD Transient Free Convection and Chemically Reactive Flow Past a Porous Vertical Plate with Radiation and Temperature Gradient Dependent Heat Source in Slip Flow Regime. IOSR Journal of Applied Physics, 3(6), pp. 22-32.

[15] Mahender D. and Rao S. P., (2015): Unsteady MHD Free Convection and Mass Transfer Flow Past a Porous Vertical Plate in Presence of Viscous Dissipation. International Conference on Vibration Problems, Journal of Physics, 662, pp. 1-7.

[16] Ahmed N., and Das K. K., (2013): MHD Mass Transfer Flow Past a Vertical Porous Plate Embedded in a Porous Medium in a Slip Flow Regime with Thermal Radiation and Chemical Reaction. Open Journal of Fluid Dynamics, 3, pp. 230-239.

[17] Rashidi M. M., Behnam R., Navid F., Saeid A., (2014): Free Convective Heat and Mass Transfer for MHD Fluid Flow Over a Permeable Vertical Stretching Sheet in the Presence of the Radiation and Buoyancy Effects. Ain Shams Engineering Journal 5, pp. 901-912.

[18] Mahbub Al Ab. Md, Nasrin J. N., Shomi A., Zillur R., (2013): Soret-Dufour Effects on the MHD Flow and Heat Transfer of Micro-rotation Fluid Over a Nonlinear Stretching Plate in the Presence of Suction. Applied Mathematics 4, pp. 864-875.

[19] Makinde O.D. and Onyejekwe (2011): A Numerical Study of MHD Generalized Couette Flow and Heat Transfer with Variable and Electrical Conductivity. Journal of Magnetism and Magnetic Materials, 323, pp. 2757-2763.

[20] Idowu A. S., Jimoh A., Oyelami F. H., Dada M. S., (2014): Numerical Solution for Thermal Radiation Effect on Inclined Magnetic Field of MHD Free Convective Heat Transfer Dissipative Fluid Flow Past a Moving Vertical Porous Plate with Variable Suction. American Journal of Fluid Dynamics, 4(3), pp. 91-101.

[21] Raju M.C., Varma S.V.K., Seshaiah B. (2015): Heat transfer effects on a viscous dissipative fluid flow past a vertical plate in the presence of inclined magnetic field. Ain Shams Engineering Journal, 6, 333-339.

[22] Ahmad N., (2011): Visco-elastic Boundary Layer Flow Past a Stretching Plate and Heat Transfer with Variable Thermal Conductivity. World Journal of Mechanics, 1, 15-20.

[23] Liao S.J. (1992): The proposed Homotopy Analysis Techinique for the Solution of Non-linear Problems. PhD dissertation, Shanghai Jiao Tong University.

[24] Motsa S.S., Sibanda P., Shateyi S. (2010): A new Spectral homotopy analysis method for solving a nonlinear second order BVP. Commun Nonlinear Science Numerical Simulation, 15, pp. 2293-2302.

[25] Makukula Z.G. and Motsa S.S., (2014): Spectral Homotopy Analysis Method for Partial differential equations that model the unsteady Von Karman Swirling Flow. Journal of Applied Fluid Mechanics, 7(4), pp. 711-718.

[26] Atabakan P. Z., Kilicman A. and Kazemi N. A., (2012): On Spectral Homotopy Analysis Method for Solving Linear Volterra and Fredholm Integro Differential Equations. Hindawi Publishing Coorporation, Abstract and Applied Analysis, doi:10.115/2012/960289, pp. 1-16.

[27] Makukula Z., Sibanda P. and Motsa S., (2010a): A note on the solution of the von Karman equations using series and chebyshev spectral methods. Hindawi Publishing Coorporation, Boundary Value Problems, Vol. 2010, doi:10.1155/2010/471793,17.

[28] Makukula Z., Sibanda P. and Motsa S.S (2010b): A novel numerical technique for two-dimensional laminar flow between two moving porous walls. Mathematical Problems in Engineering, Vol. 2010, doi:10.1155/2010/528956.

[29] Zou L., Zong Z., Dong G.H. (2008): Generalizing homotopy analysis method to solve Lotka-Volterra equation Computers and Mathematics with Applications, 56, pp. 2289-2293.

[30] Shaban M., Kazem S., Rad J.A. (2013): A Modification of the Homotopy Analysis Method Based on Chebyshev Operational Matrices. Mathematical and Computer Modelling, 57, pp. 1227-1239.

[31] Shateyi S. and Motsa S.S., (2010): Variable viscosity on Magnetohydrodynamic fluid flow and heat transfer over an unsteady stretching surface with Hall effect. Hindawi Publishing Coorporation, Boundary Value problems, pp. 1-19.

[32] Mukhopadhyay (2013): Effects of thermal radiation on casson fluid flow and heat transfer over an unsteady stretching surface subject to suction/blowing. Chinese Physical Society and IOP Publishing Ltd, 22(11), 114702-7.

[33] Fagbade A.I., Falodun B.O., Omowaye A.J. (2016). MHD natural convection flow of viscoelastic fluid over an accelerating permeable surface with thermal radiation and heat source or sink: Spectral Homotopy Analysis Approach. Ain Shams Engineering Journal (Article in Press), http://dx.doi.org/10.1016/j.asej.2016.04.021.